

# The initialization and manipulation of quantum information stored in silicon by bismuth dopants

Gavin W. Morley<sup>1,2\*</sup>, Marc Warner<sup>1,2</sup>, A. Marshall Stoneham<sup>1,2</sup>, P. Thornton Greenland<sup>1,2</sup>, Johan van Tol<sup>3</sup>, Christopher W. M. Kay<sup>1,4</sup> and Gabriel Aeppli<sup>1,2</sup>

**A prerequisite for exploiting spins for quantum data storage and processing is long spin coherence times. Phosphorus dopants in silicon (Si:P) have been favoured<sup>1–10</sup> as hosts for such spins because of measured electron spin coherence times ( $T_2$ ) longer than any other electron spin in the solid state: 14 ms at 7 K with isotopically purified silicon<sup>11</sup>. Heavier impurities such as bismuth in silicon (Si:Bi) could be used in conjunction with Si:P for quantum information proposals that require two separately addressable spin species<sup>12–15</sup>. However, the question of whether the incorporation of the much less soluble Bi into Si leads to defect species that destroy coherence has not been addressed. Here we show that schemes involving Si:Bi are indeed feasible as the electron spin coherence time  $T_2$  is at least as long as for Si:P with non-isotopically purified silicon. We polarized the Si:Bi electrons and hyperpolarized the  $I = 9/2$  nuclear spin of <sup>209</sup>Bi, manipulating both with pulsed magnetic resonance. The larger nuclear spin means that a Si:Bi dopant provides a 20-dimensional Hilbert space rather than the four-dimensional Hilbert space of an  $I = 1/2$  Si:P dopant.**

Kane's suggestion for a Si:P quantum computer<sup>1</sup>, where the electron and nuclear spins of P impurities are regulated and read out using electrical gates, has inspired many researchers. Two particular challenges in building the Kane quantum computer are placing phosphorus dopants with atomic precision<sup>2</sup> below the surface, and depositing metallic contacts between them.

Alternative schemes<sup>12–15</sup>, which are conceptually more complex but impose less stringent requirements on fabrication, take advantage of other group v elements that also substitute for silicon. With qualitatively similar behaviour to Si:P dopants, these other dopants exhibit electron spin resonance (ESR) at field/frequency combinations distinct<sup>16</sup> from Si:P, allowing selective excitation and detection with microwave pulses. As a result of their lower solubility and higher binding energies, they have been of far less relevance to microelectronics, and so in contrast to Si:P, their spin relaxation has remained relatively unexplored. This is particularly true for the heaviest element, bismuth, which has the highest binding energy and also the largest nuclear spin ( $I = 9/2$ ), both of which should be advantageous for quantum computing because they would permit higher temperature operation and a larger auxiliary state space for quantum data storage, respectively. Although Bi seems attractive in principle, a potential problem is that Bi is the largest and least soluble of the group v elements<sup>17</sup>—if the site of incorporation is too distorted or should Bi entrain other substitutional or interstitial impurities (including vacancies), extra decoherence could ensue. Accordingly, we have used pulsed ESR to measure the spin-lattice relaxation time  $T_1$  and the decoherence time  $T_2$ , as well as to

demonstrate the controlled preparation of quantum states (using Rabi oscillations) and nuclear spin manipulations using pulsed electron–nuclear double resonance (ENDOR).

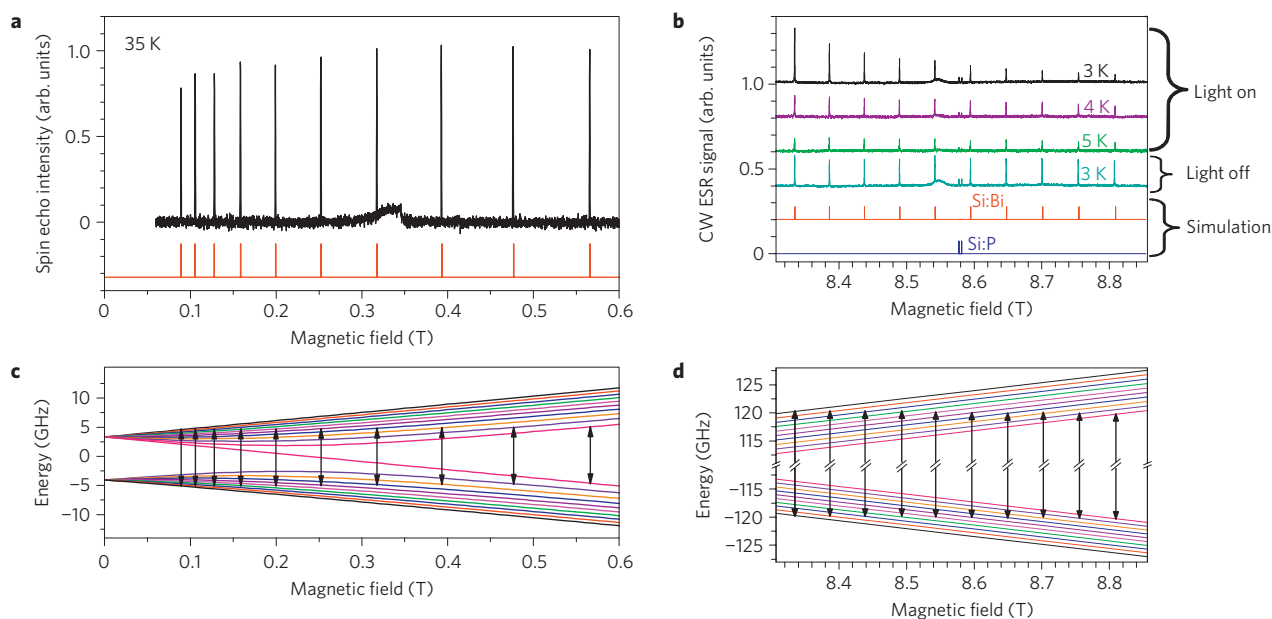
Figure 1 shows the ESR spectra obtained with both standard- (9.7 GHz) and very high- (240 GHz) frequency microwave radiation. In each case Si:Bi yields the ten resonances expected for an electron (spin 1/2) coupled to a nuclear spin of 9/2. The resonant fields of all transitions are well simulated as shown in the figure and described in the Supplementary Information. The Gaussian linewidth is shown in the Supplementary Information to be  $0.41 \pm 0.002$  mT with 9.7 GHz radiation, which agrees with the value reported previously<sup>16</sup> and attributed to interactions with the natural (4.7%) concentration of <sup>29</sup>Si nuclear spins.

Figure 1a shows a spin-echo-detected field-swept spectrum recorded with a pulsed ESR spectrometer (Bruker E580) operating at 9.7 GHz. The Supplementary Information describes in more detail all pulse sequences used in our experiments. The spectrum in Fig. 1b was recorded in continuous-wave (CW) mode at 240 GHz with a quasi-optic spectrometer<sup>18,19</sup> at the National High Magnetic Field Laboratory in Tallahassee, Florida.

For the 240 GHz experiments, a magnetic field above 8.3 T together with a temperature of 3 K ensures that the electron spin polarization is above 95%, providing a good initial state for a quantum computation using the electron spin. This almost pure state avoids the problems encountered by liquid-state NMR quantum computers with the use of pseudo-pure starting states.

In addition, we have initialized the electron–nuclear spin system by transferring some of the large electron polarization to the bismuth nuclei. Figure 1b shows that this was achieved with above-bandgap white light, without the resonant excitation used in some previous experiments<sup>10,20</sup>. This dynamic nuclear polarization is due to the Overhauser effect whereby the electron spin of the photoelectrons relaxes by 'flip-flopping' with the <sup>209</sup>Bi nuclear spin. The photoelectrons are initially unpolarized and to move towards thermal equilibrium it is necessary for ~45% of them to 'flip' spins. These flips can conserve angular momentum if a <sup>209</sup>Bi nuclear spin 'flops' in the other direction. The energy required to flop a nuclear spin is negligible compared with the thermal energy in our experiment. Very similar effects have been seen with <sup>29</sup>Si nuclear spins in silicon<sup>21</sup>, but anti-polarization occurs with Si:P (refs 6,7) owing to the trapping of conduction electrons by the P donors<sup>4</sup>. The application of light with energy only slightly larger than the bandgap can favour the formation of bound excitons in Si:Bi and a different mechanism for dynamic nuclear polarization producing anti-polarization<sup>22</sup>. The results obtained in ref. 22 came from photoluminescence measurements that are not

<sup>1</sup>London Centre for Nanotechnology, University College London, London WC1H 0AH, UK, <sup>2</sup>Department of Physics and Astronomy, University College London, London WC1E 6BT, UK, <sup>3</sup>National High Magnetic Field Laboratory and Florida State University, Tallahassee, Florida 32310, USA, <sup>4</sup>Institute of Structural and Molecular Biology, University College London, London WC1E 6BT, UK. \*e-mail: g.morley@ucl.ac.uk.



**Figure 1 | Qubit initialization.** **a,b**, ESR spectra of Si:Bi with a frequency of 9.7 GHz (**a**) and a frequency of 240 GHz (**b**). At the high magnetic field required for the higher frequency experiment, the ten Si:Bi resonances are evenly spaced (**b**). This is not the case for the lower-frequency experiment as the correspondingly lower magnetic field is not strong enough to define the axis of quantization: the large hyperfine interaction of  $a = 1.4754$  GHz (for definition, see Supplementary Information) is comparable in size to the Zeeman term in the Hamiltonian. The red lines are simulations of the Si:Bi resonances and the blue line is a simulation of the Si:P resonances that account for the sharp but weak features visible in the high-field data. In all spectra we attribute the small broad signal around  $g = 2$  (0.34 T for 9.7 GHz and 8.55 T for 240 GHz) to dangling-bond defects in the silicon.  $^{209}\text{Bi}$  nuclear polarization manifests itself in the form of a larger signal for the low-field resonance lines at temperatures below 5 K when above-bandgap light is applied. The spectra have been offset for clarity and the arbitrary units are the same for each spectrum. **c,d**, The simulated energy levels as a function of low and high magnetic field respectively, with the arrows indicating transitions that flip the electron spin state but leave the nuclear spin state unchanged.

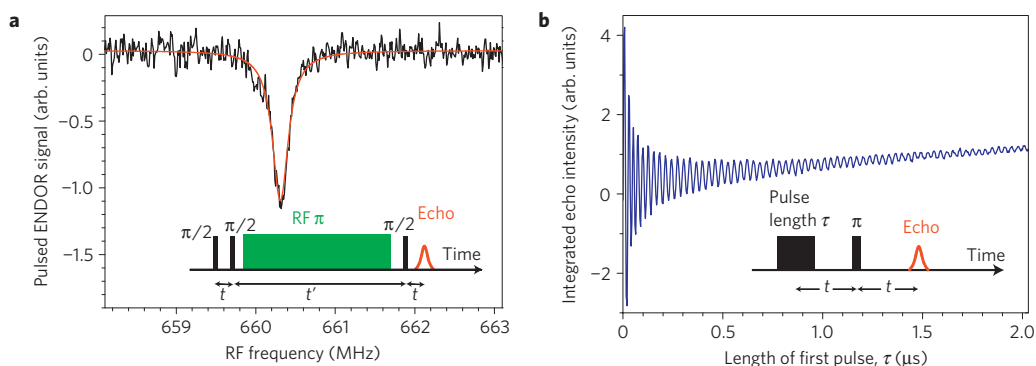


**Figure 2 | Qubit manipulation.** **a**, Pulsed ENDOR manipulates the Bi nuclear spin as well as the electron spin. A microwave frequency of 240 GHz (black rectangles in inset that control the electron spin) was used at a temperature of 3 K and the length of the radiofrequency (RF) pulse (green rectangle that controls the nuclear spin) was  $150 \mu\text{s}$ . **b**, Rabi oscillations of the electron spin at 25 K with 9.7 GHz radiation. The spin is flipped using a pulse of  $\tau = 13$  ns duration.

able to coherently manipulate spin qubits. The magnitude of the  $^{209}\text{Bi}$  nuclear polarization near the surface may be much larger than in the bulk because the light does not penetrate the entire sample<sup>6</sup>.

To use the full twenty-dimensional Hilbert space available from a Si:Bi donor for quantum computing, it is necessary not only to initialize the spin system and manipulate the electron spin, but also to manipulate the nuclear spin. To demonstrate the feasibility of this we carried out pulsed ENDOR (ref. 23) at 240 GHz, as illustrated in Fig. 2a. We fit the ENDOR resonance with a 0.24 MHz Gaussian line but this linewidth is inhomogeneous: it is not due to the nuclear relaxation times of the  $^{209}\text{Bi}$ .

To characterize the quality of our electron spin manipulations we recorded Rabi oscillations as shown in Fig. 2b, obtaining a spin

flip time of 13 ns. The characteristic timescale for the decay of these oscillations is around 100 ns, but this provides only a lower bound on the time for the decay of spin coherence.

To measure the spin coherence times of Si:Bi we recorded the electron spin echo size as a function of the separation ( $t$ ) of the  $\pi$  refocusing pulse and the initial  $\pi/2$  pulse (the inset of Fig. 3a shows the pulse sequence). For temperatures above  $\sim 18$  K the decay is exponential:  $e^{-2t/T_2}$ . The exponential decay constant for spins in a solid,  $T_m$ , is referred to here as  $T_2$  because the electron spin density is low enough that these spins interact only weakly. At lower temperatures the coherence decay is clearly non-exponential as shown in Fig. 3a. We fitted this decay with the same function<sup>8</sup> that has been used for similar experiments with

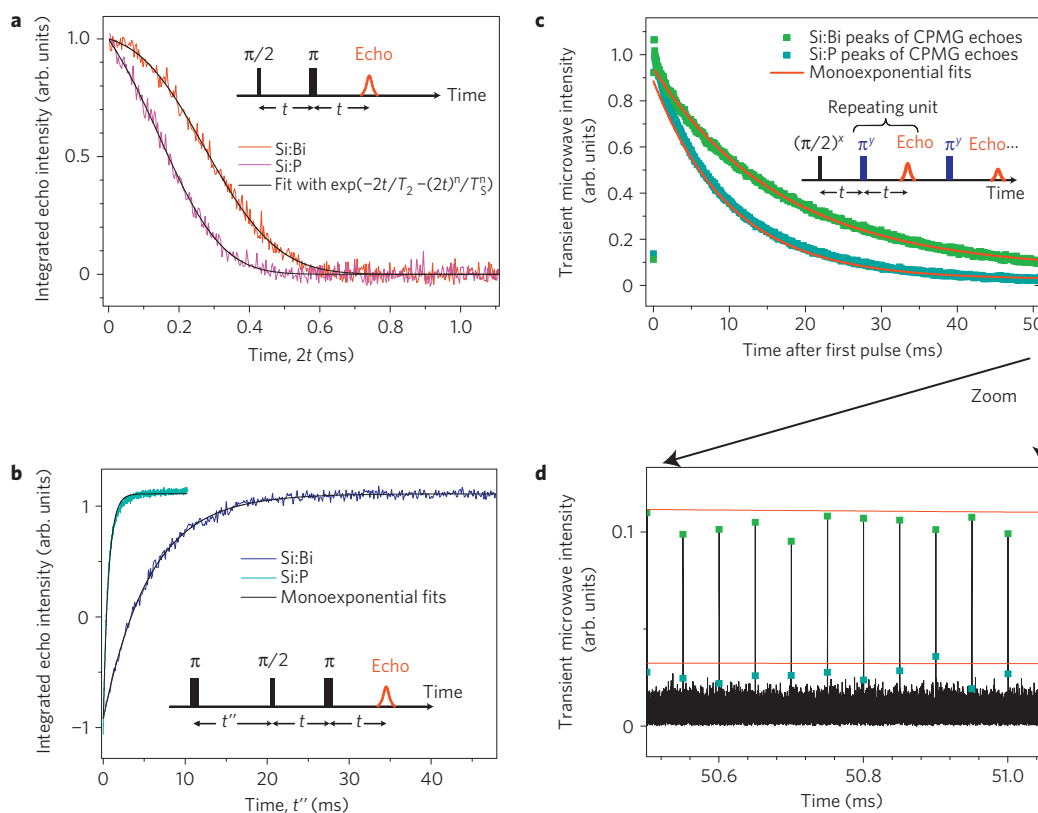


**Figure 3 | Storage of quantum information.** Electron spin relaxation of Si:Bi at 9.7 GHz, with measurements of Si:P for comparison. **a**, Spin echo decays measured at 10 K. **b**, Inversion-recovery measurements of  $T_1$  at 10 K. **c**, CPMG experiment: decay of spin echoes produced by 1,020  $\pi$  pulses at 8 K. The signal acquisition time for each sample was 20 min. **d**, Expansion of the indicated region showing the resolved echoes.

Si:P:  $e^{-2t/T_2 - (2t)^n/T_s^n}$ .  $T_s$  characterizes the coherence decay owing to the presence of  $^{29}\text{Si}$  nuclear spins. The sample was oriented with the [111] direction perpendicular to the applied magnetic field; aligning the crystal with the magnetic field along the [100] direction produces longer  $T_s$  times in Si:P experiments<sup>8,11</sup>. The best-fit value of the exponent  $n$  was between 2.5 and 2.6 for temperatures of 8–14 K. All relaxation time measurements are accompanied by directly comparable measurements of a sample of Si:P with a lower concentration of  $0.3\text{--}1 \times 10^{15} \text{ cm}^{-3}$ .

Figure 4 shows the temperature ( $T$ )-dependent  $T_2$  and  $T_s$  times. For  $T > 14$  K the spin decoherence is dominated by the spin-lattice relaxation time,  $T_1$ , which we measured with the inversion-recovery pulse sequence<sup>23</sup>. The Si:Bi inversion recoveries were well fitted by monoexponential decays such as in Fig. 3b.  $T_1$  is the typical time taken for the electron spins to polarize, and can be thought of as the timescale for storing classical information, in contrast to the quantum information storage time,  $T_2$ . As expected,  $T_1$  is dominated by phonons, but most of these have energies that are much larger than the energy gap between spin up and spin down. As a result, two-phonon processes (such as the absorption of a high-energy phonon and the emission of an even higher-energy phonon) occur more frequently than single-phonon processes. The dependence of the spin-lattice relaxation rate,  $1/T_1$ , on  $T$  is well described by an  $e^{-\Delta E/T}$  Orbach term (two-phonon process using an excited state) added to a  $T^7$  Raman term (two-phonon process using a virtual excited state). The  $\Delta E$  used in Fig. 4 was 500 K, but values from 450 to 800 K provide an acceptable fit. A value of  $\Delta E = 400$  K has previously been measured with ESR of a more concentrated sample<sup>24</sup>, and identified<sup>25</sup> with the energy gap to the  $1s(T_2)$  orbital excited state.

Si:Bi has a larger ionization energy than the other group v donors, which reduces the number of phonons with enough energy

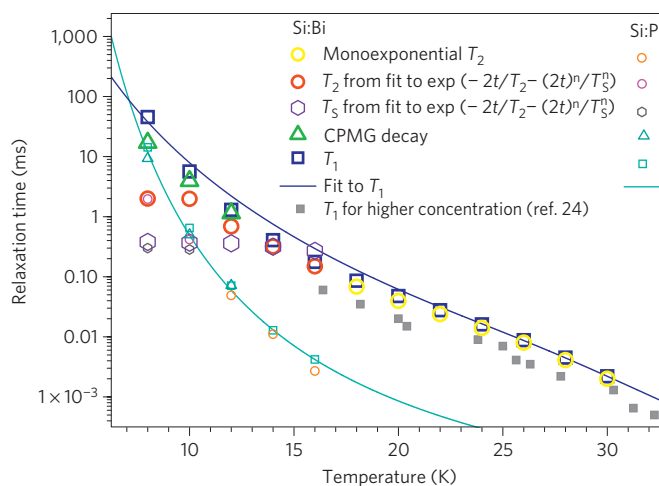


**Figure 4 | Storage times for classical ( $T_1$ ) and quantum ( $T_2$ ) information.**

Electron spin relaxation times as a function of temperature for Si:Bi, with measurements of Si:P for comparison. Our Si:Bi sample has a concentration of  $\sim 3 \times 10^{15} \text{ Bi cm}^{-3}$ . The blue squares are the  $T_1$ , the yellow circles are the monoexponential  $T_2$  values, the red circles and the purple hexagons are the  $T_2$  and  $T_s$  values respectively from the fit to the function  $e^{-2t/T_2 - (2t)^n/T_s^n}$  and the green triangles are the CPMG decays. The blue line is a fit to our  $T_1$  measurements described in the main text. For comparison, the same set of measurements with Si:P (concentration  $\sim 10^{15} \text{ cm}^{-3}$ ) is shown with smaller shapes. The grey filled squares are  $T_1$  measurements from ref. 24 for a more concentrated ( $4 \times 10^{16} \text{ cm}^{-3}$ ) sample of Si:Bi.

to access the excited  $1s(T_2)$  states where two-phonon Orbach spin-lattice relaxation occurs strongly<sup>25</sup>. This means that in the

temperature regime where Orbach effects dominate, the  $T_1$  time of Bi is longer than all other group v donors in Si (ref. 24). The  $T_1$  times measured here follow the same temperature dependence as those in ref. 24, but the higher spin concentration of  $4 \times 10^{16} \text{ cm}^{-3}$  used in that work led to shorter relaxation times. A similar concentration-dependent effect has been described for Si:P (ref. 26).

For temperatures below 14 K, the spin echo decay in Si:Bi is limited by the 4.7% of Si nuclei with spin 1/2 that provide the  $T_S$  decay. With an isotopically pure sample of  $^{28}\text{Si}:\text{Bi}$  this contribution would not have been present, revealing the magnitude of other interactions such as the weak dipolar coupling to other Si:Bi electron spins. To remove some of the effects of the  $^{29}\text{Si}$  decoherence at temperatures between 8 and 12 K, we applied a train of 1,020  $\pi$  pulses<sup>23,27</sup> (Fig. 3c). With this Carr–Purcell–Meiboom–Gill (CPMG) sequence, sources of decoherence can be dynamically decoupled, including not only the coupling to  $^{29}\text{Si}$  nuclei, but also instrumental imperfections in the spectrometer.

The CPMG decay at 8 K shown in Fig. 3c has an exponential decay time of 17 ms. Some CPMG decays have been attributed to a collective response of spin ensembles to  $\pi$  pulses that are not short enough<sup>28</sup>. We consider this possibility in the Supplementary Information. The CPMG decays we measure in Si:P are shorter than for Si:Bi in our temperature range, and limited by the  $T_1$  time. The  $T_2$  time of isotopically pure  $^{28}\text{Si}:\text{P}$  has been measured<sup>11</sup> as 14 ms at 6.9 K with a Hahn echo sequence, the longest electron spin  $T_2$  time in the literature for a solid-state system. A Hahn echo decay of 1.8 ms has been reported for the nitrogen–vacancy centre in diamond<sup>29</sup>; this measurement was at room temperature but required isotopically pure diamond and there is no deterministic fabrication paradigm here to rival those already working in silicon<sup>2</sup>. Furthermore, although the diamond results were obtained with a single electron spin, electrical detection is moving in the direction of single electron spin readout of donors in silicon<sup>4,9</sup>. The differing resonant frequencies of dopants in slightly different environments may permit selective addressing<sup>13</sup>. Our results are clearly sufficiently promising to warrant the fabrication of high-quality crystals of isotopically pure  $^{28}\text{Si}:\text{Bi}$ . Such a sample would be particularly exciting in light of a presentation at a recent workshop<sup>30</sup> reporting an unpublished measurement of  $T_2 = 0.6 \text{ s}$  for isotopically purified  $^{28}\text{Si}:\text{P}$ . In analogy with the observations in  $^{28}\text{Si}:\text{P}$ , the Si:Bi  $T_2$  should increase towards the limiting value of  $2T_1$ .

The very long spin coherence times we measure show that Si:Bi is well suited for storing quantum information. We have flipped the electron spin in a time of 13 ns, and find  $T_2 = 2 \text{ ms}$ : over  $10^5$  times longer. We conclude that quantum information processing in silicon can be based not only on phosphorus dopants, but also bismuth dopants and combinations of the two, as required in schemes<sup>13,15</sup> where the dopants with higher binding energies function as qubits and the others are the control bits, regulated for example by terahertz radiation<sup>5</sup>.

*Note added in proof:* We discuss some of the extra possibilities for Si:Bi quantum information processing in ref 31. Also, while carrying out further experiments and preparing our manuscript for resubmission following initial refereeing, an online preprint appeared reporting pulsed ESR and ENDOR of bismuth dopants in non-isotopically purified silicon with low magnetic fields of up to 0.6 T (ref. 32).

## Methods

The samples used here are single float-zone crystals of silicon, bulk doped in the melt with bismuth atoms. A  $2 \times 2 \times 4 \text{ mm}$  sample with a concentration estimated as  $3 \times 10^{15} \text{ Bi cm}^{-3}$  was used for the 9.7 GHz measurements, whereas a  $\sim 4 \times 10^{14} \text{ Bi cm}^{-3}$  sample ( $1 \times 2 \times 4 \text{ mm}$ ) was used for the measurements at 240 GHz. For the pulsed ENDOR measurement (Fig. 2a) we applied white light to shorten the electron spin  $T_1$  time<sup>26</sup>, enabling a shorter shot repetition time. The same light source was used in Fig. 1b.

The highest field ESR resonance was used for all of the relaxation times presented here, and short (16 ns)  $\pi/2$  pulses were used to excite the entire EPR resonance. To measure the Hahn echo decays (such as Fig. 3a), single shots were collected and the magnitudes of the echo signals were averaged<sup>8,11,18</sup>. Our calibrated Cernox thermometer was used to control the temperature to  $\pm 0.1 \text{ K}$ .

Received 15 July 2009; accepted 6 July 2010; published online 15 August 2010

## References

- Kane, B. E. A silicon-based nuclear spin quantum computer. *Nature* **393**, 133–137 (1998).
- Schofield, S. R. *et al.* Atomically precise placement of single dopants in Si. *Phys. Rev. Lett.* **91**, 136104 (2003).
- Morton, J. J. L. *et al.* Solid-state quantum memory using the P-31 nuclear spin. *Nature* **455**, 1085–1088 (2008).
- Morley, G. W. *et al.* Long-lived spin coherence in silicon with an electrical spin trap readout. *Phys. Rev. Lett.* **101**, 207602 (2008).
- Greenland, P. T. *et al.* Coherent control of Rydberg states in silicon. *Nature* **465**, 1057–1061 (2010).
- McCamey, D. R., van Tol, J., Morley, G. W. & Boehme, C. Fast nuclear spin hyperpolarization of phosphorus in silicon. *Phys. Rev. Lett.* **102**, 027601 (2009).
- van Tol, J. *et al.* High-field phenomena of qubits. *Appl. Magn. Res.* **36**, 259–268 (2009).
- Tyryshkin, A. M. *et al.* Coherence of spin qubits in silicon. *J. Phys. Condens. Matter* **18**, S783–S794 (2006).
- Morello, A. *et al.* Single-shot readout of an electron spin in silicon. Preprint at <http://arxiv.org/abs/1003.2679> (2010).
- Yang, A. *et al.* Subsecond hyperpolarization of the nuclear and electron spins of phosphorus in silicon by optical pumping of exciton transitions. *Phys. Rev. Lett.* **102**, 257401 (2009).
- Tyryshkin, A. M., Lyon, S. A., Astashkin, A. V. & Raitsimring, A. M. Electron spin relaxation times of phosphorus donors in silicon. *Phys. Rev. B* **68**, 193207 (2003).
- Benjamin, S. C. Quantum computing without local control of qubit–qubit interactions. *Phys. Rev. Lett.* **88**, 017904 (2002).
- Stoneham, A. M., Fisher, A. J. & Greenland, P. T. Optically driven silicon-based quantum gates with potential for high-temperature operation. *J. Phys. Condens. Matter* **15**, L447–L451 (2003).
- Benjamin, S. C. & Bose, S. Quantum computing with an always-on Heisenberg interaction. *Phys. Rev. Lett.* **90**, 247901 (2003).
- Stoneham, A. M., Harker, A. H. & Morley, G. W. Could one make a diamond-based quantum computer? *J. Phys. Condens. Matter* **21**, 364222 (2009).
- Feher, G. Electron spin resonance experiments on donors in silicon. I. Electronic structure of donors by the electron nuclear double resonance technique. *Phys. Rev.* **114**, 1219–1244 (1959).
- Pajot, B. & Stoneham, A. M. A spectroscopic investigation of the lattice distortion at substitutional sites for group V and group VI donors in silicon. *J. Phys. C* **20**, 5241–5252 (1987).
- Morley, G. W., Brunel, L.-C. & van Tol, J. A multifrequency high-field pulsed electron paramagnetic resonance/electron-nuclear double resonance spectrometer. *Rev. Sci. Instrum.* **79**, 064703 (2008).
- van Tol, J., Brunel, L. C. & Wylde, R. J. A quasioptical transient electron spin resonance spectrometer operating at 120 and 240 GHz. *Rev. Sci. Instrum.* **76**, 074101 (2005).
- Morley, G. W. *et al.* Efficient dynamic nuclear polarization at high magnetic fields. *Phys. Rev. Lett.* **98**, 220501 (2007).
- Lampel, G. Nuclear dynamic polarization by optical electronic saturation and optical pumping in semiconductors. *Phys. Rev. Lett.* **20**, 491–493 (1968).
- Sekiguchi, T. *et al.* Hyperfine structure and nuclear hyperpolarization observed in the bound exciton luminescence of Bi donors in natural Si. *Phys. Rev. Lett.* **104**, 137402 (2010).
- Schweiger, A. & Jeschke, G. *Principles of Pulse Electron Paramagnetic Resonance* (Oxford Univ. Press, 2001).
- Castner, T. G. Direct measurement of the valley-orbit splitting of shallow donors in silicon. *Phys. Rev. Lett.* **8**, 13–15 (1962).
- Castner, T. G. Orbach spin-lattice relaxation of shallow donors in silicon. *Phys. Rev.* **155**, 816–825 (1967).
- Feher, G. & Gere, E. A. Electron spin resonance experiments on donors in silicon II. Electron spin relaxation effects. *Phys. Rev.* **114**, 1245–1256 (1959).
- Du, J. F. *et al.* Preserving electron spin coherence in solids by optimal dynamical decoupling. *Nature* **461**, 1265–1268 (2009).
- Li, D. *et al.* Intrinsic origin of spin echoes in dipolar solids generated by strong  $\pi$  pulses. *Phys. Rev. B* **77**, 214306 (2008).
- Balasubramanian, G. *et al.* Ultralong spin coherence time in isotopically engineered diamond. *Nature Mater.* **8**, 383–387 (2009).

30. Tyryshkin, A. M. & Lyon, S. A. Data presented at the Silicon Qubit Workshop 24–25 August (Univ. California, sponsored by Lawrence Berkeley National Laboratory and Sandia National Laboratory, 2009).
31. Mohammadi, H. M., Morley, G. W. & Monteiro, T. S. Bismuth qubits in silicon: the role of EPR cancellation resonances. *Phys. Rev. Lett.* (in the press); preprint at <http://arxiv.org/abs/1004.3475> (2010).
32. George, R. E. *et al.* Electron spin coherence and electron nuclear double resonance of Bi donors in natural Si. *Phys. Rev. Lett.* (in the press); preprint at <http://arxiv.org/abs/1004.0340> (2010).

### Acknowledgements

We thank B. Pajot for supplying the Si:Bi samples. Our research was supported by the RCUK Basic Technologies programme, the EPSRC programme grant COMPASS and a Wolfson Royal Society Research Merit Award. The National High Magnetic Field

Laboratory is supported by NSF Cooperative Agreement No. DMR-0654118, and by the State of Florida. G.W.M. is supported by an 1851 Research Fellowship.

### Author contributions

G.W.M., M.W. and C.W.M.K. carried out the experiments at 9.7 GHz; G.W.M. and J.v.T. carried out the experiments at 240 GHz. G.W.M. and P.T.G. carried out the simulations. G.W.M. analysed the data, which were interpreted by G.W.M., A.M.S., J.v.T., C.W.M.K. and G.A. The Letter was written by G.W.M., A.M.S., J.v.T., C.W.M.K. and G.A.

### Additional information

The authors declare no competing financial interests. Supplementary information accompanies this paper on [www.nature.com/naturematerials](http://www.nature.com/naturematerials). Reprints and permissions information is available online at <http://npg.nature.com/reprintsandpermissions>. Correspondence and requests for materials should be addressed to G.W.M.